Using Local Volume data to constrain Dark Matter dynamics

G. Lavaux (lavaux@iap.fr), R. Mohayaee, S. Colombi, R. B. Tully

Institut d'Astrophysique de Paris, 98bis Bd Arago, 75014 PARIS, FRANCE

CNRS/Université Pierre et Marie Curie

I will present here the Monge-Ampère-Kantorovitch peculiar velocity reconstruction method applied to mock catalogues mimicking some observational biases encountered in real life. The method is then applied to a 3000 km/s deep galaxy catalogue to recover the peculiar velocities of these galaxies in our neighbourhood.

I. Introduction

Objective: Recovering individual velocities of galaxies from their redshift position $\mathbf{z} = H\mathbf{x} + \mathbf{v}\cdot\frac{\mathbf{x}}{||\mathbf{x}||}$, with $\mathbf{x}$ its comoving position, $\mathbf{v}$ its velocity, H the Hubble constant. Comparison to larger Local Volume measurements may yield new constraints on M/Ls.

Poster is organized as follows:

- Short presentation of the Monge-Ampère-Kantorovitch Lagrangian reconstruction method + Algorithm.
- Test on large-scale simulations.
- Two examples of observation biases to which the method is sensitive:
  - Catalogue geometry limited by visibility of objects → general boundary problem (limited access to gravity field and velocity field variance).
  - Unknown distribution of the diffuse mass (*i.e.* $M \lesssim 10^{11-12}$ M$_\odot$).
- A direct application to NBG-3k follows, which shows the reconstructed velocities in our neighbourhood.

II. The Monge-Ampère-Kantorovitch (MAK) reconstruction

Theory

Motivation: Zel'dovich approximation (Zel'Dovich, 1970), which is the first development order in the Lagrangian perturbation theory, works really well on Large scales. It leads to considering the displacement field of the dark matter from initial conditions is deriving from a convex potential. We remind that in general Zeldovich approximation writes $\mathbf{x}(\mathbf{q},t) = \mathbf{q} + D(t)\mathbf{\Psi}(\mathbf{q})$, with $\mathbf{x}$ the current position, $\mathbf{q}$ the initial position, $D(t)$ the linear growth factor.

Hypothesis: the displacement field traced by galaxies is deriving from a convex potential.

Problem: Find the corresponding displacement field given an initial (homogeneous) density field and the current observable density field.

⇒ Brenier et al. (2003) shown that the minimization of

$$S_\sigma = \sum_{i=0}^{N}\left(\mathbf{x}_i - \mathbf{q}_{\sigma(i)}\right)^2 \qquad (1)$$

according to σ solves the above problem, with i representing an homogeneous sampling of the mass distribution, where the $\mathbf{x}_i$ are the current positions of these particles, and the $\mathbf{q}_j$ are distributed on a regular grid. An illustration of the minimization is given Fig. 1.

⇒ i-th velocity recovered using Zel'dovich approximation

$$v_i = \beta\Psi_i \text{ with } \beta \equiv \Omega_{\mathrm{m}}^{5/9} \qquad (2)$$

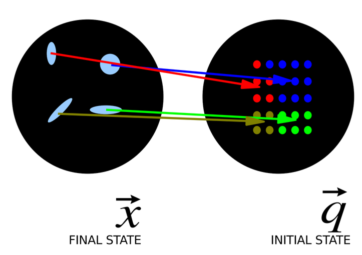

Figure 1: Minimization process: galaxies are pictured on the left and their corresponding Lagrangian domain is on the right ($\mathbf{q}$s)

Algorithm

Minimization of Eq. (1) is a computationally difficult problem (time complexity $O(N!)$) → in Bertsekas (1979), "Auction" algorithm is minimizing cost-flow problems and can be adapted to minimization of Eq. (1) ⇒ Time complexity in $O(N^{2.25})$. Particles i, put at $\mathbf{x}_i$, compete against other particle j to acquire the Lagrangian position $\mathbf{q}_k$. k is given to i if it represents the best assignment globally. When the equilibrium is reached, the current assignment corresponds to the solution of minimizing Eq. (1). However efficiency depends a lot on the degeneracy of the solution.

Implementation

On Dual-core AMD Athlon64 4800+, SMP implementation: 79,000 particles ⇔ 50 mins. A MPI version of the corresponding algorithm has also been implemented but only performant for sufficiently large number of particles or denser problems ($N/V \gtrsim 1\,h$Mpc^{-3}).

III. Application to cosmological simulation

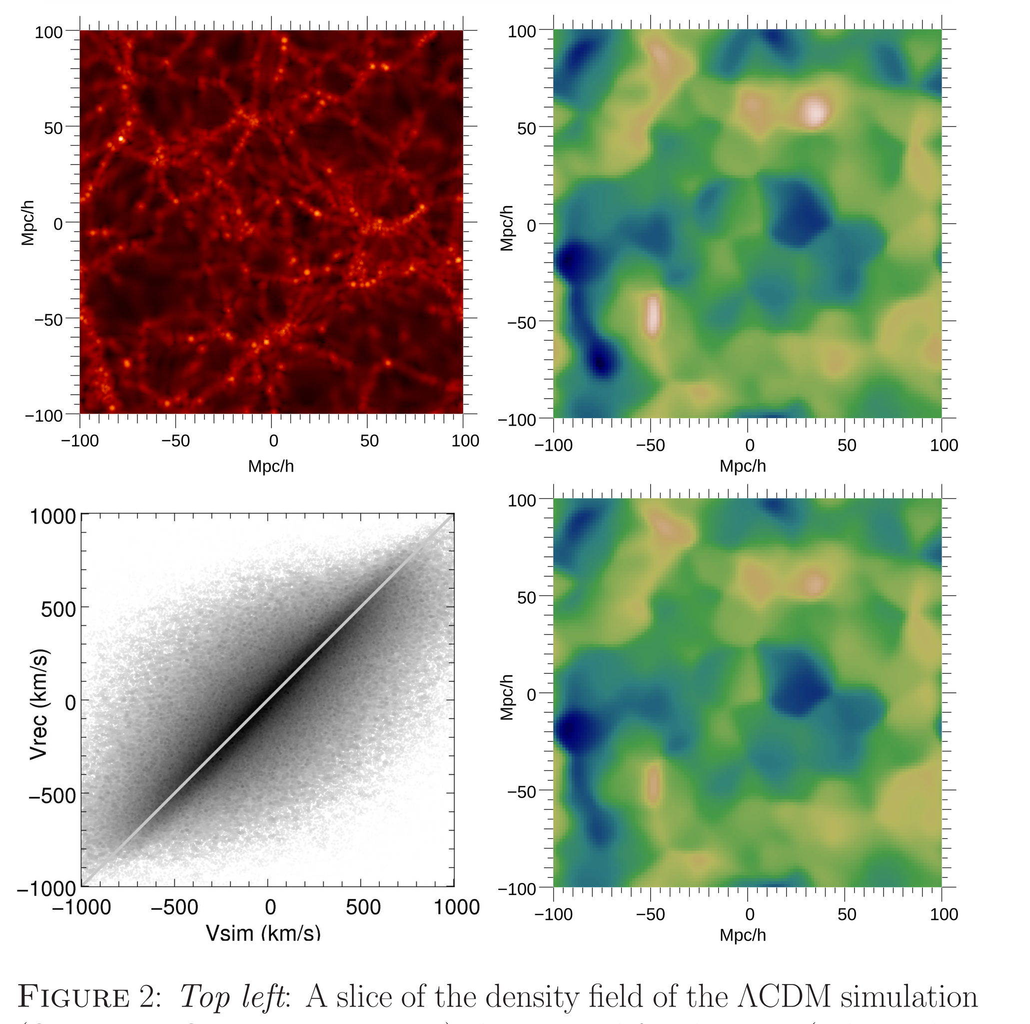

Figure 2: *Top left*: A slice of the density field of the ΛCDM simulation ($\Omega_{\mathrm{m}} = 0.30, \Omega_\Lambda = 0.70, \sigma_8 = 1.0$) that is used for the tests (color coding in log scale). *Top right*: Velocity field of the same slice. *Bottom right*: MAK reconstructed velocity field of the same slice. Linear color scale: dark blue=-1000 km.s^{-1}, white=+1000 km.s^{-1}. *Bottom left*: Scatter distribution while comparing $P(v_r, v_{\mathrm{sim}})$ of the individual objects velocity fields in the right column. (color coding in log scale). The reconstruction is actually giving the right velocity field above 3-5 h^{-1}Mpc.

IV. Outer boundary / Recovering Lagrangian domain

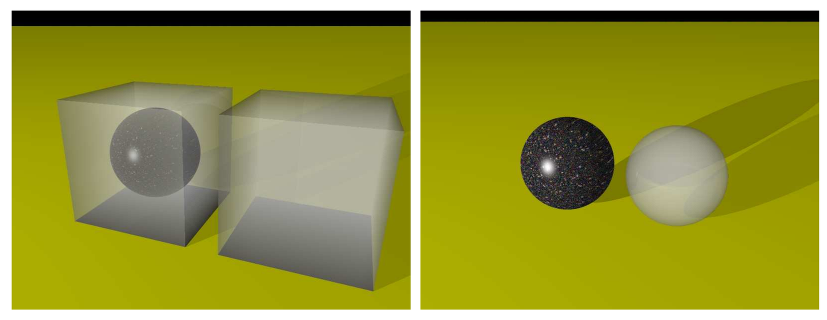

Figure 3: Reconstruction setup when one does not know the Lagrangian domain $\mathbf{q}$ of a catalogue of mass tracers (ball painted with galaxies). *Left (NaiveDom MAK reconstruction)*: One assumes that the geometry of the catalogue is conserved between $t = 0$ and $t = t_0$. The MAK reconstruction is achieved between the catalogue and the right crystal sphere. *Right (PaddedDom MAK recontruction)*: The catalogue is padded homogeneously to smooth out boundary effects (crystal box). The padded catalogue is MAK reconstructed using the the right crystal box.

Finite volume catalogues ⇒ unknown Lagrangian volume (⇔ unknown large scale tidal fields) ⇒ miss-reconstruction of trajectories of galaxies.

Screening of the gravitational field by fluctuations of the density field has 2 consequences:

⊕ Different correction scheme to handle edge effects should not cause disturbance at the center of the catalogue.

⊖ Buffer zone between mis-reconstructed MAK solution (due to edge effects) and the unaffected solution may be big (> 20 Mpc/h).

Proposed solution: Padding the original "spherical" catalogue as illustrated in Fig. 3 and assuming a cubic Lagrangian domain of the same size → Real space reconstruction results are given in Fig. 5.

Result: Given in Fig. 4. The central part of the velocity field is well reconstructed in both cases (NaiveDom and PaddedDom). Individual velocity comparison shows that NaiveDom is still a worse boundary condition than PaddedDom.

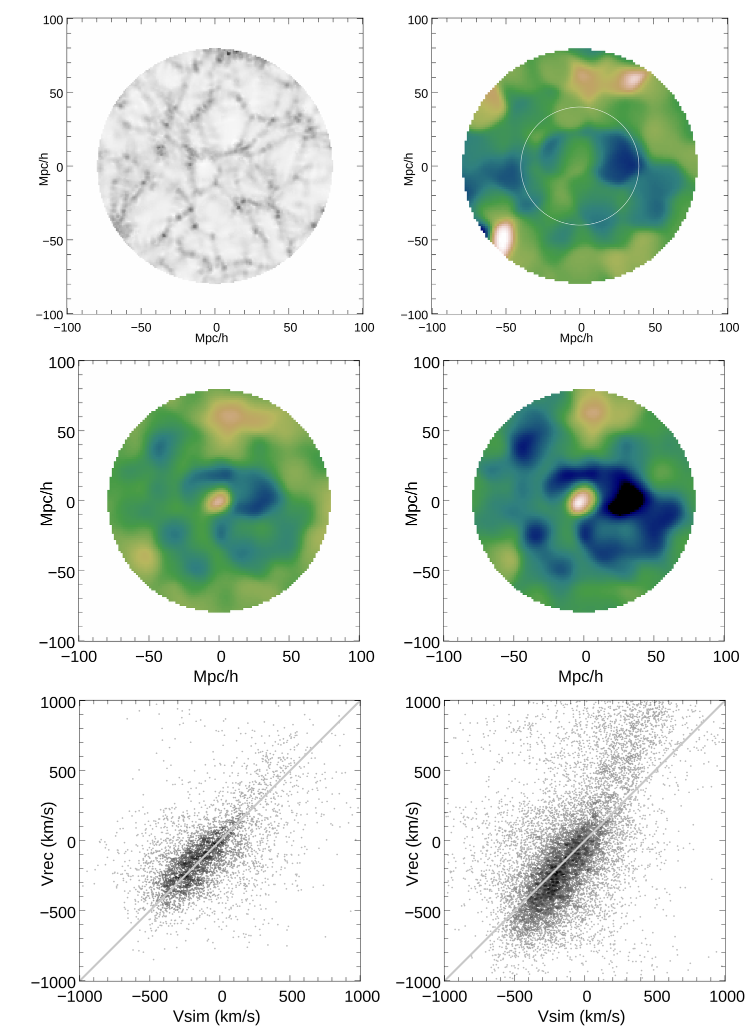

Figure 4: Outer boundary problems while doing reconstruction on finite volume catalogue. Color scale is the same everywhere (dark blue=-1000 km/s, white=+1000 km/s). *Top left*: Density field of the mock catalogue (log scale). *Top right*: Simulated velocity field, smoothed with a 5 Mpc/h Gaussian window. *White circle:* Volume enclosed by the 40 Mpc/h sphere centered on the observer. *Middle left*: PaddedDom velocity field, smoothed equally. *Middle right*: NaiveDom velocity field, smoothed equally. The two lower panels give the catter plots of reconstructed velocities *vs* simulated velocities. Only objects inside the white circles have been represented. *Lower left:* NaiveDom redshift reconstruction. *Right:* PaddedDom redshift reconstruction.

V. Undetected diffuse mass

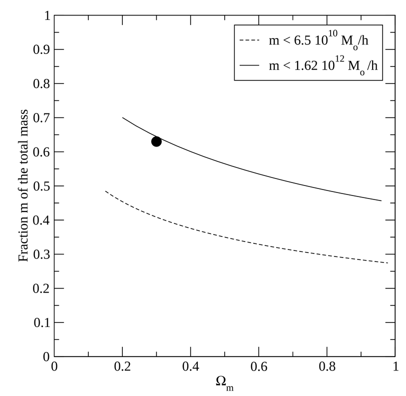

Figure 5: *Diffuse mass* – In this plot, we represent the fraction of the clustered mass below two mass resolution for WMAP1 type cosmology ($h = 0.72, \sigma_8 = 0.9$). A BBKS power spectrum has been used. The curvature of the Universe is kept flat while Ω_{m} varies. This fraction is plotted for two mass resolution: 2×10^{12} M$_\odot$ and 10^{11} M$_\odot$ ($\simeq 5\times10^9$ L$_\odot$). The fraction of mass below both of these limits is still considerable.

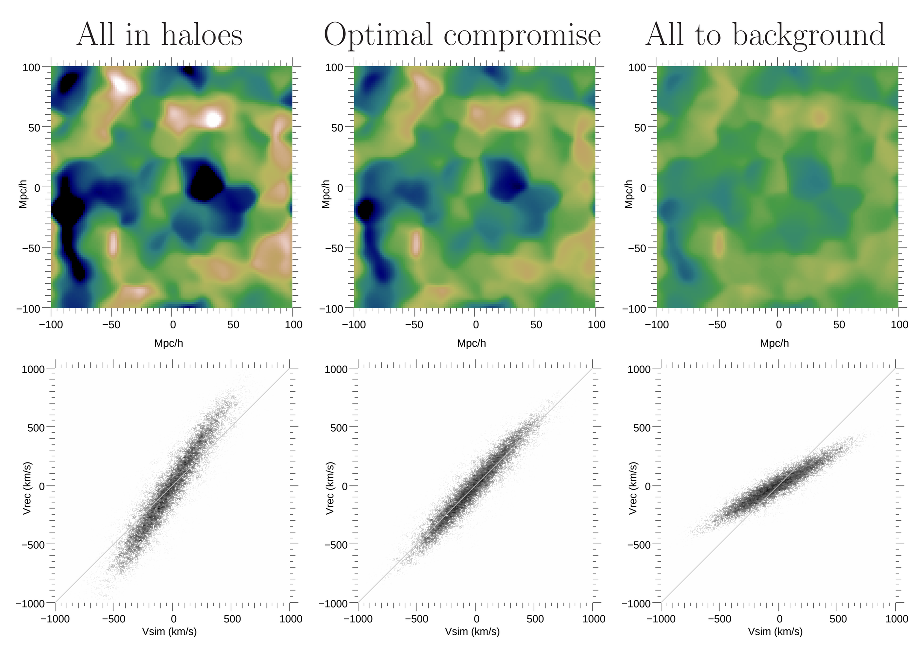

Figure 6: Here mock catalogues are separated in two phases: the halo catalogue ($M \geq 1.62\times10^{12}$M$_\odot$) and the background field ($M < 1.62\times10^{12}$M$_\odot$) representing 63% of the total mass. The higher row of panels represents the line-of-sight component of a slice of the reconstructed velocity field, smoothed in the same way, for different correction of the diffuse mass. The lower row of panels give the scatter distribution of individual reconstructed velocities of haloes *vs* simulated ones. *Left panels:* Result of a reconstruction on a mock catalogue which only contains the haloes and not the background field but at the same time conserves the total mass of the catalogue by reassigning the missing mass to the haloes. *Right panels:* Result for a reconstruction with a background field composed of particles placed randomly in the catalogue. *Center panels:* Result when one tries to find a optimal compromise between distributing the missing mass in haloes and randomly in the background field (here 60% in haloes and the rest in the background).

VI. Direct Application to NBG-3k (Tully et al., 2007)

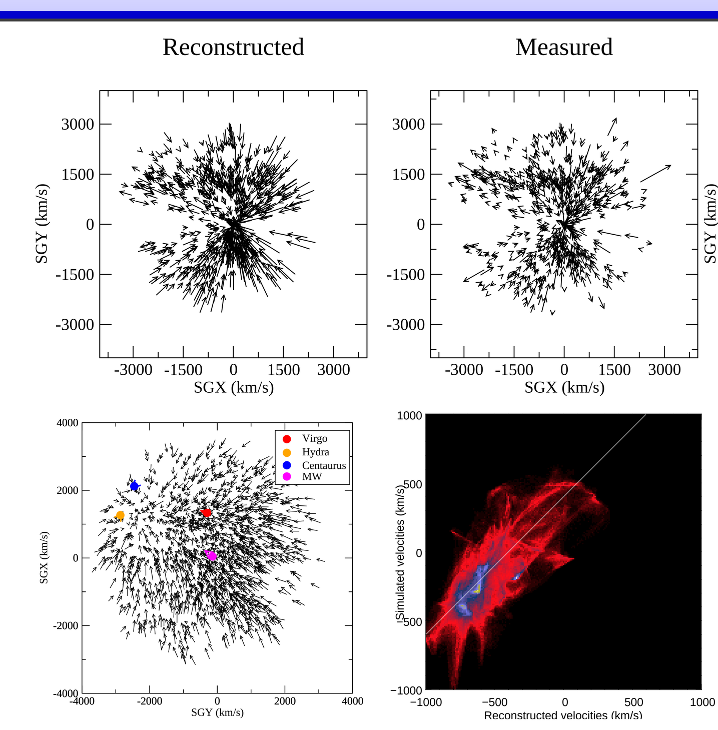

Figure 7: *Top panels:* Reconstructed and measured individual velocities. This is a ***preliminary*** result and β measurement is likely to be still biased at the moment. *Lower left:* 3D velocities projected along the SGZ axis. *Lower right:* Scatter plot showing that the reconstructed displacement field Ψ_{rec} is really correlated with the one obtained through direct measurements V_{mes}. We remind that the displacement field is proportional to the velocity field in Zel'dovich approximation. However, a spurious offset is still present.

This reconstructed velocities has been produced assuming

$$\left(\frac{M}{L}\right)_{\mathrm{spiral}} = 100\frac{\mathrm{M}_\odot}{\mathrm{L}_\odot} \text{ and } \left(\frac{M}{L}\right)_{\mathrm{elliptical}} = 300\frac{\mathrm{M}_\odot}{\mathrm{L}_\odot} \qquad (3)$$

for objects of the NBG-3k catalogue.

VII. Conclusion

- Results:
  - Simple padding scheme shows that velocities may be correctly reconstructed (but a buffer zone of 20 Mpc/h is needed).
  - Diffuse mass may be accounted for but more tests on different cosmlogical simulations are needed to calibrate the way this mass is partitioned between haloes and background.
- Problems & Perspective
  - Look for better M/Ls to have a higher correlation between reconstructed and measured velocities.
  - Better velocity reconstruction by integrating more non-linearities due to gravitation along trajectories (*i.e.* solving exactly the Euler-Poisson problem, in preparation).

References

Bertsekas D. P., 1979, A Distributed Algorithm for the Assignment Problem. MIT Press, Cambridge, MA

Brenier Y., Frisch U., Hénon M., Loeper G., Matarrese S., Mohayaee R., Sobolevskiĭ A., 2003, MNRAS, 346, 501

Shaya E. J., Peebles P. J. E., Tully R. B., 1995, ApJ, 454, 15

Tully R. B., Shaya E. J., Karachentsev I. D., Courtois H., Kocevski D. D., Rizzi L., Peel A., 2007, ArXiv e-prints, 705

Zel'Dovich Y. B., 1970, A&A, 5, 84